

# Graphene Films Show Stable Cell Attachment and Biocompatibility with Electrogenic Primary Cardiac Cells

Taeyong Kim<sup>1</sup>, Yung Ho Kahng<sup>2,\*</sup>, Takhee Lee<sup>3</sup>, Kwanghee Lee<sup>2</sup>, and Do Han Kim<sup>1,\*</sup>

**Graphene has attracted substantial attention due to its advantageous materialistic applicability. In the present study, we tested the biocompatibility of graphene films synthesized by chemical vapor deposition with electrogenic primary adult cardiac cells (cardiomyocytes) by measuring the cell properties such as cell attachment, survival, contractility and calcium transients. The results show that the graphene films showed stable cell attachment and excellent biocompatibility with the electrogenic cardiomyocytes, suggesting their useful applications for future cell biology studies.**

## INTRODUCTION

Since graphene was discovered in 2004, it has attracted substantial research interest in materials science, because of its superior characteristics such as mechanical and chemical robustness, mechanical flexibility, large surface area, chemical functionalization capability, and excellent electrical conductivity (Geim, 2009; Geim and Novoselov, 2007). A primary goal of graphene film applied research has been to develop transparent electrodes for optoelectronic devices (Jo et al., 2010a; 2010b; Lee et al., 2011). Recently, biomedical applications of graphene films has attracted considerable attention (Bitounis et al., 2013; Cohen-Karni et al., 2010; Duch et al., 2011; Hess et al., 2011; Li et al., 2011; Mao et al., 2013; Sahni et al., 2013).

Graphene consists of  $sp^2$  hybridization-bonded carbon atoms in a hexagonal lattice structure. It is important to investigate the utility of graphene in biological systems, because carbon is the backbone of most biological molecules. Graphene research has concentrated on subjects such as biosensors, drug delivery, antimicrobials, tissue engineering, and biocompatibility (Bitounis et al., 2013; Cohen-Karni et al., 2010; Duch et al., 2011; Hess et al., 2011; Jang et al., 2013; Li et al., 2011; Mao et al., 2013; Sahni et al., 2013). Biomedical applications of graphene are at an early stage of development. Because of its unique properties such as large surface area, electrical conductivity, flexibility,

and transparency, graphene could be utilized as scaffolds for cell growth, electrical lead materials for cell activation by devices such as pacemakers, and biosensors (Cohen-Karni et al., 2010; Hess et al., 2011; Li et al., 2011). Investigating the biocompatibility of graphene with electrogenic cells is a prerequisite to understanding the broad applicability of graphene in biomedical applications. Most previous studies of graphene biocompatibility with cells have used chemically modified graphene, which has poorer electrical conductance than graphene synthesized by chemical vapor deposition (CVD) (Bitounis et al., 2013; Duch et al., 2011). Most previous reports also studied immortalized cell lines, which may not show physiological responses that are comparable to *in vivo* responses to graphene (Bitounis et al., 2013; Hess et al., 2011). Therefore, it is important to test the biocompatibility of CVD graphene films with electrically excitable cells such as cardiomyocytes.

A few studies have addressed the *in vitro* biocompatibility of CVD graphene with primary neuronal cells or embryonic cardiomyocytes by assessing cell viability, morphology, and other properties (Cohen-Karni et al., 2010; Li et al., 2011; Sahni et al., 2013), but to our knowledge, primary adult cardiomyocytes have never been tested for biocompatibility with graphene. The major differences between embryonic and adult cardiomyocyte are in 1) differentiation and proliferation, 2) cellular structure such as sarcomere structure and sarcoplasmic reticulum and 3) expression level of important signaling molecules. Embryonic cardiomyocytes are undifferentiated proliferating cells, while adult cardiomyocytes are fully differentiated and show little or no proliferation. Since the sarcomere and sarcoplasmic reticulum structures of embryonic cardiomyocytes are not fully developed, the contractile functions and calcium dynamics of them are distinct compared with the adult ones. In the case of the receptor-mediated cardiac signaling, one good example is that the  $\beta$ -adrenergic receptor isoforms are differentially expressed between embryonic and adult cardiomyocytes. In addition, because adult cardiomyocytes are much more sensitive than embryonic or neonatal cardiomyocytes to stresses such as pH change and oxidative stress, it is important to investigate the

<sup>1</sup>School of Life Sciences and Systems Biology Research Center, <sup>2</sup>Research Institute for Solar and Sustainable Energies (RISE), Gwangju Institute of Science and Technology (GIST), Gwangju 500-712, Korea, <sup>3</sup>Department of Physics and Astronomy, Seoul National University, Seoul 151-747, Korea  
\*Correspondence: yhkahng@gist.ac.kr (YHK); dhkim@gist.ac.kr (DHK)

Received October 7, 2013; revised October 31, 2013; accepted November 4, 2013; published online November 29, 2013

**Keywords:** calcium transients, chemical vapor deposition, cytotoxicity, excitable cells, graphene

biocompatibility of adult cardiomyocytes with graphene substrates.

In this study, we explored the biocompatibility of CVD graphene with primary cardiomyocytes with respect to cell attachment, survival rates, and two physiological responses (contractility and calcium transient). The tested properties were similar or superior to those of cardiomyocytes grown on a reference glass substrate, suggesting that CVD graphene substrates are excellent vehicles for future studies of electrogenic cells such as cardiomyocytes.

## MATERIALS AND METHODS

### Substrate preparation

CVD graphene was synthesized as reported previously (Kahng et al., 2011; Lee et al., 2011). Briefly, graphene was synthesized on Si/SiO<sub>2</sub> (300 nm)/Ti (20 nm)/Ni (300 nm) substrates purchased from Jinsol, Inc. Graphene films were synthesized in a CVD chamber with flow rates of 1.6 sccm (standard cubic centimeters per minute) methane, 208 sccm hydrogen, and 192 sccm argon for 5 min at 1,000°C and 760 Torr. Following synthesis, the graphene films were transferred from the nickel substrate by etching the nickel in an aqueous iron chloride (FeCl<sub>3</sub>) solution (1 M). Next, the graphene films were cleaned 3 times in DI (deionized) water. During transfer, a polymethylmethacrylate (PMMA) coating was applied as a protective layer and then removed with acetone after transfer. After cleaning, graphene films were transferred to glass coverslips. The graphene coated glass coverslips were incubated with 11 µg/ml laminin (BD Biosciences) in phosphate buffered saline solution at 37°C for 3 h. Prior to plating cardiomyocytes, the laminin solution was removed.

### Atomic force microscopy

The atomic force microscope (AFM) used in this study was an XE-100 system from Park Systems, Inc. AFM scans were performed with a typical scan rate of 0.5 Hz in non-contact mode.

### Scanning electron microscopy

Cardiomyocytes plated on graphene + laminin- or laminin-coated coverslips were fixed with 4% (w/v) paraformaldehyde at room temperature for 1 h. After several washes with phosphate buffered saline, the cells were dehydrated using an ethanol gradient and coated with 2 nm of platinum for 60 s. Finally, the cells were examined with a Hitachi S-4700 field emission scanning electron microscope (FESEM) operating with an accelerating voltage of 10 kV.

### Isolation and culture of adult rat ventricular myocytes

Adult rat ventricular myocytes were isolated from adult (10-14-week-old) male Sprague-Dawley rats using a previously described procedure with minor modifications (Kwon and Kim, 2009). Hearts were excised from anesthetized (isoflurane inhalation) adult rats, mounted on a Langendorf apparatus, and perfused through the aorta (retrograde) with oxygenated Ringer's solution of the following composition: 125 mM NaCl, 5 mM KCl, 25 mM HEPES, 2 mM KH<sub>2</sub>PO<sub>4</sub>, 1.2 mM MgSO<sub>4</sub>, 5 mM pyruvate, 11 mM glucose, 5 mM creatine, 5 mM L-carnitine, and 5 mM taurine (pH 7.4 adjusted with NaOH). Initial perfusion was for 5 min with Ringer's solution containing 1 mM CaCl<sub>2</sub> followed by another perfusion with calcium-free Ringer's solution for 15 min. Calcium-free Ringer's solution containing 230 U/ml collagenase type 2 (Worthington) and 0.4 mg/ml hyaluronidase (Sigma) was recirculated through the heart for 30 min,

followed by a final 1 min perfusion with Ringer's solution containing 4% BSA (Bovogen) and 10 mM 2,3-butanedione monoxime (Sigma). The cannulus was removed from the heart and the ventricles were cut away and diced.

After myocytes were filtered through a 100 µm Cell Strainer (BD Biosciences), CaCl<sub>2</sub> was added to the final concentration of 1.8 mM, and they were incubated for 10 min. Myocytes were plated on 11 µg/ml laminin (BD Biosciences)-coated glass coverslips or coverslips coated first with graphene and then with laminin at a density of 10<sup>4</sup> cells/cm<sup>2</sup> and incubated at 37°C and 5% CO<sub>2</sub> in M199 medium (Sigma) containing 25 mM HEPES, 2.2 g/L antibiotics (Gibco), 2.5 mM taurine, 2.5 mM carnitine, and 2.5 mM creatine. After incubating for 2 h, unattached cells were removed by washing with the same media.

All animal experiments were carried out in accordance with the Gwangju Institute of Science and Technology Animal Care and Use Committee guidelines.

### Differential interference contrast (DIC) microscopy

To assess cardiomyocyte viability, cells in live culture were imaged using an LSM 700 confocal laser-scanning microscope (Carl Zeiss, Co.). Images were obtained under a ×10 objective lens at 5, 19, and 24 h after cell plating.

### Cell contractility and intracellular Ca<sup>2+</sup> transient measurements

The mechanical properties of cardiomyocytes were assessed using the video-based edge detection system (IonOptix) as previously described (Oh et al., 2012; Park et al., 2013) but with minor modifications. Cardiomyocytes were incubated with 2 µM Fura2-AM (Invitrogen), a Ca<sup>2+</sup>-sensitive indicator, for 15 min at room temperature to load the indicator into the cytosol. Cells were then washed with tyrode solution for 15 min and field-stimulated at a frequency of 1 Hz (30 V). Changes in cell length during shortening and relengthening were captured for 20 s (20 traces for each cell) and analyzed using soft edge software (IonOptix). While being stimulated to contract, cardiomyocytes were exposed to light emitted by a 75 W xenon lamp through either a 340 or 380 nm excitation filter. Fluorescence emission was detected at 480-520 nm with a photomultiplier tube after initial illumination at 340 nm for 0.5 s and then at 380 nm for the duration of the recording protocol. The 340 nm excitation scan was repeated at the end of the protocol, and qualitative changes in the intracellular Ca<sup>2+</sup> concentration were inferred from the ratio of Fura2-AM fluorescence intensity at both excitation wavelengths. Approximately 20 cells plated on each laminin-coated coverslip (n = 5) and laminin-coated graphene coverslip (n = 3) were chosen for contractility and Ca<sup>2+</sup> transient measurements. The composition of the tyrode solution used for Fura2-AM loading was as follows: 125 mM NaCl, 5 mM KCl, 25 mM HEPES, 2 mM KH<sub>2</sub>PO<sub>4</sub>, 1.2 mM MgSO<sub>4</sub>, 5 mM pyruvate, 11 mM glucose, and 2 mM CaCl<sub>2</sub> (pH 7.4 adjusted with NaOH).

### Statistical analysis

Results from at least 3 independent experiments were expressed as the mean ± standard error of the mean. Comparisons between groups were performed by the Student's 2-tailed t-test for experiments. Probability values less than 0.05 were considered statistically significant. All analyses were performed with SigmaPlot 12 software (Systat Software, Inc.).

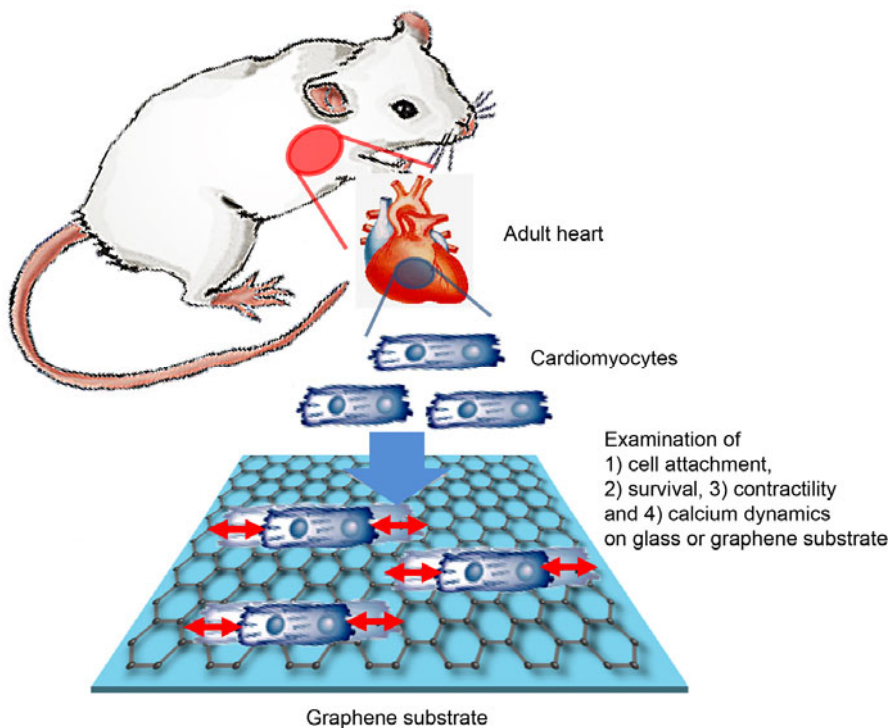


**Fig. 1.** Schematic drawings of the present experimental protocols. The primary cardiac cells were extracted from heart of anesthetized rats. The cardiac cells underwent various experimental protocols to evaluate their physiological parameters on laminin-coated glass or laminin-coated graphene.

## RESULTS AND DISCUSSION

### Laminin coating on graphene

Laminin is a large (900 kDa) cruciform protein ubiquitously found in the basement membranes of extracellular matrices (Beck et al., 1990). Laminin provides structural support for various cell types, thereby enabling their proper organization into various organs (Yarnitzky and Volk, 1995). Laminin is required for cell attachment in primary cultures of cardiomyocytes (Bird et al., 2003). Thus, the effect of a laminin coating on graphene, and any interactions between the two, had to be investigated in order to characterize graphene as a potential biomedical material for the culture of cardiac tissue or cardiomyocytes.

Glass coverslips were prepared with 4 different specifications: (i) pristine, (ii) laminin coated on pristine, (iii) graphene deposited, and (iv) laminin coated on graphene. To analyze the surface property of each substrate, AFM images (Fig. 2) and the root mean square (RMS) measurements of roughness were obtained. These images show the differences between pristine and graphene-deposited coverslips before and after laminin coating. On pristine coverslips, the laminin coat showed dense formation of laminin aggregates that were several tens of nanometers both in width and height, and sporadic formation of larger laminin aggregates that were hundreds of nanometers both in width and height (Fig. 2B). The surface roughness increased significantly from 0.48 nm for the pristine coverslip to 31.9 nm for the laminin-coated coverslip, indicating substantial laminin aggregation on glass coverslips. In contrast, the small laminin aggregates formed more sparsely on the graphene-deposited coverslips than on the glass coverslips, and the large laminin aggregates were not observed (Fig 2D). The RMS roughness of the graphene-deposited coverslips increased from 5.2 nm without laminin coating to 11.2 nm with laminin coating, showing a smaller difference than seen without graphene. The

smaller increase in roughness indicates that a smaller amount of laminin was deposited on the graphene substrate than on the glass substrate. The lower deposition of hydrophilic laminin aggregates on the graphene substrate compared to glass may be due to the higher hydrophobicity of graphene compared to glass. Despite the sparse formation, the aggregated laminins were clearly observed on the graphene-coated coverslips (Fig. 2D). The observation of laminin attachment indicates that graphene can be mixed with hydrophilic substrates (e.g., poly-L-lysine and gelatin) and used for cell cultures. A previous report described the use of graphene mixed with poly-L-lysine for culturing nerve cells (Li et al., 2011).

The surface properties of the laminin substrate can be changed by different coating conditions (e.g., pH), which can affect cell morphology and physiology (Freire et al., 2002). Our AFM images showed a distinct change in the coated laminin morphology because of graphene. Therefore, cell viability and physiology should be investigated on laminin-coated graphene substrates rather than laminin-coated glass substrates.

### Cell viability of cardiomyocytes on graphene

It has been reported that graphene substrates exhibit biocompatibility with live cell cultures (Cohen-Karni et al., 2010; Duch et al., 2011; Hess et al., 2011; Li et al., 2011; Sahni et al., 2013). However, primary adult cardiomyocytes have never been evaluated for biocompatibility with graphene substrates. In this study, the viability of cardiomyocytes on graphene substrates was assessed by counting live cardiomyocytes on each substrate. Because cardiomyocytes did not attach significantly to glass or graphene substrates without laminin coating, laminin-coated glass or graphene substrates were used for all experiments. The DIC micrographs (Figs. 3B and 3C) showed that cell viability of cardiomyocytes on graphene substrates was similar to glass substrates. In order to systemically investigate

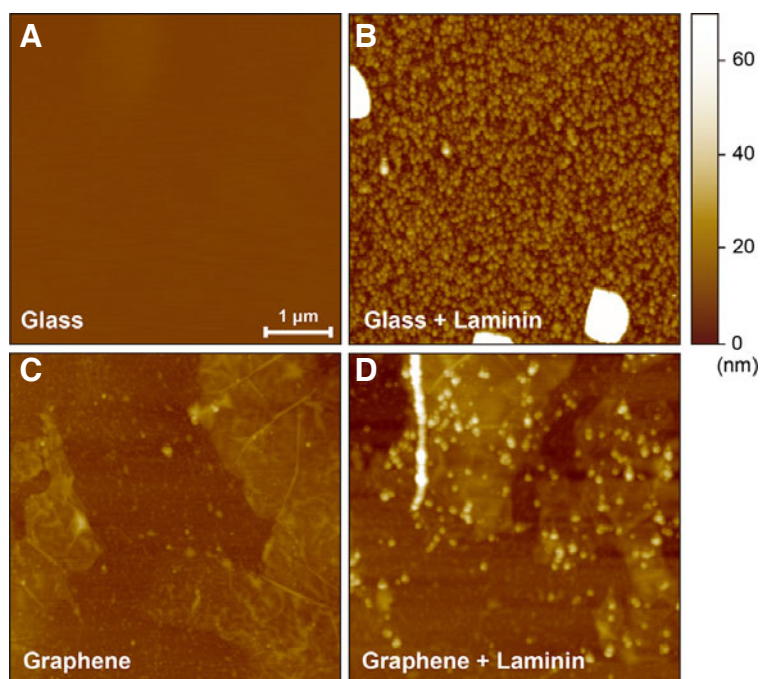


**Fig. 2.** AFM images of glass, laminin-coated glass, graphene and laminin-coated graphene substrates. The images from glass substrates without (A) and with laminin coating (B) are shown. Images from graphene substrates without (C) and with laminin coating (D) are presented. The lateral scale bar shown in (A) represents 1  $\mu\text{m}$ . The scale bars are the same for all images.

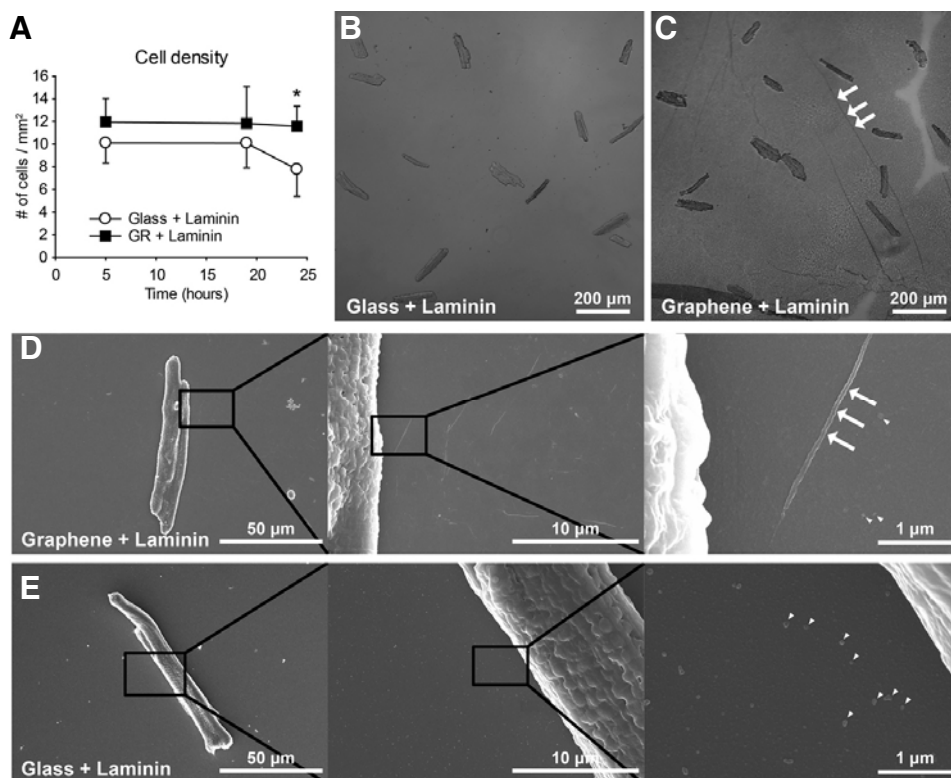


**Fig. 3.** Morphological features of cardiomyocytes on laminin-coated glass and laminin-coated graphene. Adult rat cardiomyocytes were isolated and plated on a laminin-coated glass substrate (B, E) and a laminin-coated graphene substrate (C, D). (A) The time-dependent cell viability on both substrates. Cell viability of rat adult cardiomyocytes on graphene or glass substrate was observed. Data are expressed as the mean  $\pm$  S.E.M.,  $n \geq 5$ .  $*p < 0.05$  with Student's *t*-test. (B) A representative DIC image of cardiomyocytes plated on a glass substrate. (C) A representative DIC image of cardiomyocytes plated on a graphene substrate. Graphene film shows ripple formations (white arrows), typically observed on CVD graphene. (D) A series of FESEM images of a cardiomyocyte on graphene with increasing magnifications. The latter image shows ripple formations (white arrows) and laminin aggregates (arrow heads). (E) A

series of FESEM images of a cardiomyocyte plated on glass substrate. The images show laminin aggregates (arrow heads).

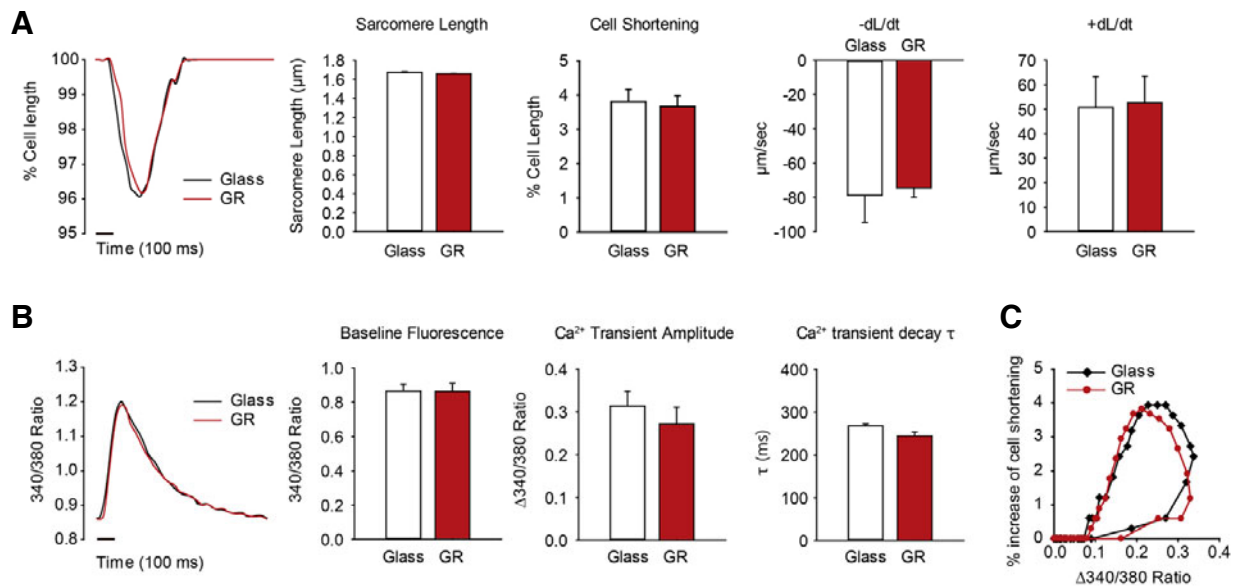


**Fig. 4.** Measured physiological parameters of cardiomyocytes attached on glass or graphene substrate. (A) Contractility of rat adult cardiomyocytes plated on glass or graphene. Graphs show a representative contraction trace, sarcomere length, peak cell shortening, percentage of shortened cell length,  $-dL/dt$  (maximal rate of cell shortening), and  $+dL/dt$  (maximal rate of cell relengthening). (B) Calcium transient properties determined by using fura2-AM. The graphs show the representative calcium transients traces, baseline intracellular calcium levels, calcium transient amplitudes, and  $\tau$  (calcium transient decay rate) for cardiomyocytes plated on glass and graphene substrates. (C) Two representative plots of the hysteresis loop of cell shortening versus cytosolic calcium content are shown. Approximately 20 cells plated on each laminin-coated coverslip ( $n = 5$ ) or laminin-coated graphene coverslip ( $n = 3$ ) were chosen for contractility and  $Ca^{2+}$  transient measurements. All data are expressed as the mean  $\pm$  S.E.M.

the cell viability, time-dependent cell densities were measured at 5, 19, and 24 h after plating on each substrate (Fig. 3A). Cell densities on the graphene substrate ( $12.0 \pm 2.1$  cells/mm<sup>2</sup> at 5 h and  $11.8 \pm 3.2$  cells/mm<sup>2</sup> at 19 h) were comparable to the glass substrate ( $10.1 \pm 1.8$  cells/mm<sup>2</sup> at 5 h and  $10.1 \pm 2.2$  cells/mm<sup>2</sup> at 19 h). However, at 24 h the graphene substrate showed a significantly higher cell density ( $11.6 \pm 1.8$  cells/mm<sup>2</sup>) than the glass substrate ( $7.8 \pm 2.4$  cells/mm<sup>2</sup>;  $p < 0.05$ ), implying that the graphene substrate was not only compatible with cardiomyocytes, but also might have improved the attachment of cardiomyocytes.

This result is consistent with the previous report showing that graphene oxide film exhibited remarkably higher cell growth of fibroblasts compared to glass substrate (Ryoo et al., 2010). Even though it is still unclear how carbon-based nanomaterial-coated substrates have higher cell holding/scaffolding capacity, expression levels of focal adhesion proteins (eg. talin or vinculin) are presumed to be related to the phenomenon. Another possibility is the surface wettability which is determined by surface chemistry, roughness and texture; the difference of surface wettability between substrates may affect the cell attachment through ionic force or an alteration in the adsorption of conditioning molecules (Kalbacova et al., 2010). High resolution FESEM images of cardiomyocytes on graphene (Fig. 3D) and glass (Fig. 3E) substrates showed similar cell integrity and cell attachment on both substrates.

#### Physiology of cardiomyocytes on graphene

To further analyze physiological responses of cardiomyocytes on graphene, we measured their calcium dynamics and contractility. After isolated adult rat cardiomyocytes were plated on

laminin-coated graphene substrates and laminin-coated glass substrates, contractile properties were measured. Glass substrate coverslips have been widely used as the general substrate for various microscopic imaging experiment (e.g. calcium imaging) (Park et al., 2013; Yoon et al., 2008). The sarcomere length and all the contractile parameters, cell shortening, rates of contraction ( $-dL/dt$ ), and rates of relaxation ( $+dL/dt$ ), were similar both for cells plated on graphene and glass substrates (Fig. 4A). Contraction rates were  $-0.79 \pm 0.16$   $\mu\text{m/s}$  for graphene and  $-0.74 \pm 0.06$   $\mu\text{m/s}$  for glass, and relaxation rates were  $0.51 \pm 0.13$   $\mu\text{m/s}$  for graphene and  $0.53 \pm 0.11$   $\mu\text{m/s}$  for glass. Since contractile parameters show the state of cardiomyocyte health, this result suggests that cardiomyocytes plated on the graphene substrate are functionally intact.

Calcium transient, an important function of cardiomyocytes, was measured along with contractility. There were no significant differences in the intracellular diastolic calcium concentrations (Baseline Fluorescence), the amplitude of  $Ca^{2+}$  transient, or the time constant of  $Ca^{2+}$  transient decay ( $\tau$ ) between the two groups (Fig. 4B). Cell shortenings were plotted against cytosolic  $Ca^{2+}$  contents during steady-state contractions (Fig. 4C). There was no distinguishable difference between the hysteresis curves of the cardiomyocytes on graphene and glass substrates. Impaired calcium transient is a key feature of altered excitation-contraction coupling, which leads to contractile dysfunction, cardiac arrhythmias, and cardiac failure (Gregory et al., 2006; Yamamoto et al., 1999). The similar calcium transient parameters for cardiomyocytes plated on the graphene substrate compared with the reference suggest that the functional activity of cardiomyocytes was not affected by the graphene substrates. Taken together, we conclude that graphene is a biocompatible

substrate for cardiomyocytes, because the physiological responses of intracellular calcium transient, contractility and calcium sensitivity were similar for rat adult cardiomyocytes both on graphene substrates and glass substrates.

This study demonstrates that graphene substrates exhibit excellent biocompatibility with primary adult rat cardiomyocytes. Cell viability on graphene substrates was comparable or superior to that on reference glass substrates. Calcium dynamics and contractility were comparable in cells grown on both substrates. Given the fact that adult cardiomyocytes are fairly sensitive to stresses under *in vitro* conditions, our results suggest that the graphene substrates are excellent supports for the biological cells from various tissue origins.

## ACKNOWLEDGMENTS

This work was supported by the 2013 GIST Systems Biology Infrastructure Establishment Grant and the Core Technology Development Program for Next-Generation Solar Cells of the Research Institute for Solar and Sustainable Energies (RISE) at Gwangju Institute of Science and Technology (GIST).

## REFERENCES

- Beck, K., Hunter, I., and Engel, J. (1990). Structure and function of laminin: anatomy of a multidomain glycoprotein. *FASEB J.* *4*, 148-160.
- Bird, S.D., Doevendans, P.A., van Rooijen, M.A., Brutel de la Riviere, A., Hassink, R.J., Passier, R., and Mummery, C.L. (2003). The human adult cardiomyocyte phenotype. *Cardiovasc. Res.* *58*, 423-434.
- Bitounis, D., Ali-Boucetta, H., Hong, B.H., Min, D.H., and Kostarelos, K. (2013). Prospects and challenges of graphene in biomedical applications. *Adv. Mater.* *25*, 2258-2268.
- Cohen-Karni, T., Qing, Q., Li, Q., Fang, Y., and Lieber, C.M. (2010). Graphene and nanowire transistors for cellular interfaces and electrical recording. *Nano Lett.* *10*, 1098-1102.
- Duch, M.C., Budinger, G.R., Liang, Y.T., Soberanes, S., Urich, D., Chiarella, S.E., Campochiaro, L.A., Gonzalez, A., Chandel, N.S., Hersam, M.C., et al. (2011). Minimizing oxidation and stable nanoscale dispersion improves the biocompatibility of graphene in the lung. *Nano Lett.* *11*, 5201-5207.
- Freire, E., Gomes, F.C., Linden, R., Neto, V.M., and Coelho-Sampaio, T. (2002). Structure of laminin substrate modulates cellular signaling for neuritogenesis. *J. Cell Sci.* *115*, 4867-4876.
- Geim, A.K. (2009). Graphene: status and prospects. *Science* *324*, 1530-1534.
- Geim, A.K., and Novoselov, K.S. (2007). The rise of graphene. *Nat. Mater.* *6*, 183-191.
- Gregory, K.N., Ginsburg, K.S., Bodi, I., Hahn, H., Marreez, Y.M., Song, Q., Padmanabhan, P.A., Mitton, B.A., Waggoner, J.R., Del Monte, F., et al. (2006). Histidine-rich Ca binding protein: a regulator of sarcoplasmic reticulum calcium sequestration and cardiac function. *J. Mol. Cell Cardiol.* *40*, 653-665.
- Hess, L.H., Jansen, M., Maybeck, V., Hauf, M.V., Seifert, M., Stutzmann, M., Sharp, I.D., Offenhausser, A., and Garrido, J.A. (2011). Graphene transistor arrays for recording action potentials from electrogenic cells. *Adv. Mater.* *23*, 5045-5049, 4968.
- Jang, H., Ryoo, S.R., Lee, M.J., Han, S.W., and Min, D.H. (2013). A new helicase assay based on graphene oxide for anti-viral drug development. *Mol. Cells* *35*, 269-273.
- Jo, G., Choe, M., Cho, C.Y., Kim, J.H., Park, W., Lee, S., Hong, W.K., Kim, T.W., Park, S.J., Hong, B.H., et al. (2010a). Large-scale patterned multi-layer graphene films as transparent conducting electrodes for GaN light-emitting diodes. *Nanotechnology* *21*, 175201.
- Jo, G., Na, S.-I., Oh, S.-H., Lee, S., Kim, T.-S., Wang, G., Choe, M., Park, W., Yoon, J., Kim, D.-Y., et al. (2010b). Tuning of a graphene-electrode work function to enhance the efficiency of organic bulk heterojunction photovoltaic cells with an inverted structure. *Appl. Phys. Lett.* *97*, 213301.
- Kahng, Y.H., Lee, S., Choe, M., Jo, G., Park, W., Yoon, J., Hong, W.K., Cho, C.H., Lee, B.H., and Lee, T. (2011). A study of graphene films synthesized on nickel substrates: existence and origin of small-base-area peaks. *Nanotechnology* *22*, 045706.
- Kalbacova, M., Broz, A., Kong, J., and Kalbac, M. (2010). Graphene substrates promote adherence of human osteoblasts and mesenchymal stromal cells. *Carbon* *48*, 4323-4329.
- Kwon, S.J., and Kim, D.H. (2009). Characterization of junctate-SERCA2a interaction in murine cardiomyocyte. *Biochem. Biophys. Res. Commun.* *390*, 1389-1394.
- Lee, S., Jo, G., Kang, S.J., Wang, G., Choe, M., Park, W., Kim, D.Y., Kahng, Y.H., and Lee, T. (2011). Enhanced charge injection in pentacene field-effect transistors with graphene electrodes. *Adv. Mater.* *23*, 100-105.
- Li, N., Zhang, X., Song, Q., Su, R., Zhang, Q., Kong, T., Liu, L., Jin, G., Tang, M., and Cheng, G. (2011). The promotion of neurite sprouting and outgrowth of mouse hippocampal cells in culture by graphene substrates. *Biomaterials* *32*, 9374-9382.
- Mao, X., Su, H., Tian, D., Li, H., and Yang, R. (2013). Bipyrene-functionalized graphene as a "turn-on" fluorescence sensor for manganese(II) ions in living cells. *ACS Appl. Mater. Interfaces* *5*, 592-597.
- Oh, J.G., Jeong, D., Cha, H., Kim, J.M., Lifirsu, E., Kim, J., Yang, D.K., Park, C.S., Kho, C., Park, S., et al. (2012). PICOT increases cardiac contractility by inhibiting PKCzeta activity. *J. Mol. Cell Cardiol.* *53*, 53-63.
- Park, C.S., Chen, S., Lee, H., Cha, H., Oh, J.G., Hong, S., Han, P., Ginsburg, K.S., Jin, S., Park, I., et al. (2013). Targeted ablation of the histidine-rich Ca(2+)-binding protein (HRC) gene is associated with abnormal SR Ca(2+)-cycling and severe pathology under pressure-overload stress. *Basic Res. Cardiol.* *108*, 344.
- Ryoo, S.R., Kim, Y.K., Kim, M.H., and Min, D.H. (2010). Behaviors of NIH-3T3 fibroblasts on graphene/carbon nanotubes: proliferation, focal adhesion, and gene transfection studies. *ACS Nano* *4*, 6587-6598.
- Sahni, D., Jea, A., Mata, J.A., Marcano, D.C., Sivaganesan, A., Berlin, J.M., Tatsui, C.E., Sun, Z., Luerssen, T.G., Meng, S., et al. (2013). Biocompatibility of pristine graphene for neuronal interface. *J. Neurosurg. Pediatr.* *11*, 575-583.
- Yamamoto, T., Yano, M., Kohno, M., Hisaoka, T., Ono, K., Tanigawa, T., Saiki, Y., Hisamatsu, Y., Ohkusa, T., and Matsuzaki, M. (1999). Abnormal Ca<sup>2+</sup> release from cardiac sarcoplasmic reticulum in tachycardia-induced heart failure. *Cardiovasc. Res.* *44*, 146-155.
- Yarnitzky, T., and Volk, T. (1995). Laminin is required for heart, somatic muscles, and gut development in the *Drosophila embryo*. *Dev. Biol.* *169*, 609-618.
- Yoon, J., Choi, S.C., Park, C.Y., Choi, J.H., Kim, Y.I., Shim, W.J., and Lim, D.S. (2008). Bone marrow-derived side population cells are capable of functional cardiomyogenic differentiation. *Mol. Cells* *25*, 216-223.